

Interacting Bose gases in twisted-bilayer optical lattices

Ganesh C. Paul,¹ Patrik Recher,^{1,2} and Luis Santos³

¹*Institut für Mathematische Physik, Technische Universität Braunschweig, D-38106 Braunschweig, Germany*

²*Laboratory for Emerging Nanometrology Braunschweig, D-38106 Braunschweig, Germany*

³*Institut für Theoretische Physik, Leibniz Universität, 30167 Hannover, Germany*

(Dated: July 17, 2025)

Recent experiments have realized ultra-cold gases in twisted-bilayer optical lattices. We show that interacting bosons in these lattices present a highly non-trivial ground-state physics resulting from the interplay between inter- and intra-layer hopping and interactions. This physics is crucially determined by site clusterization, which we properly take into account by developing a specifically-tailored cluster Gutzwiller approach. Clusterization results in a large variety of different Mott-like phases characterized by typically different occupations of the clusters, and in the appearance of pockets of sites in between which particles can freely move, but which remain disconnected from each other. This peculiar phase, which resembles the well-known Bose glass phase, may occur even for commensurate twist angles and is further enhanced when the twisting is incommensurate. Moreover, in the incommensurate case, the formation of mobility islands may occur even without inter-layer hopping solely due to inter-layer interactions.

I. INTRODUCTION

Recent years have witnessed major breakthroughs in solid state studies of twisted-bilayer materials and moiré physics [1–3], including the observation of anomalous superconductivity [4–7] and insulating behavior [8–11]. Whereas at magic commensurate twisting angles a periodic superlattice (moiré) modulation develops [1], at incommensurate twistings the system presents quasi-disorder, resembling quasicrystals [12].

Recently, ultracold atoms in optical potentials have been revealed as a suitable platform for the quantum simulation of twisted-bilayer physics [13–19]. Twisted-bilayer square lattices using two coupled internal states as effective bilayers in a synthetic dimension [13] have been recently realized by employing atomic Bose–Einstein condensates loaded into spin-dependent optical lattices [20]. Optical lattice experiments, which are characterized by an exquisite experimental control of all relevant parameters (most relevantly the interparticle interactions, hopping amplitudes, and the lattice geometry) open exciting perspectives for the study of the properties of interacting particles in twisted potentials.

Short-range interacting bosons in regular periodic lattices present as a function of the chemical potential and hopping rate, either a superfluid or a Mott insulator phase in the ground-state [21]. The presence of disorder or quasi-disorder results in the appearance of the Bose glass (BG) [22–24], an insulator which, in contrast to the Mott phase, presents a finite compressibility. Recently, Bose glasses have been discussed in the context of quasi-crystalline structures [25–27], including single-layer twisted potentials, where weak superfluidity was reported for commensurate angles [28]. Very recently, it was shown that bosons in twisted-bilayer optical lattices may present in the absence of interlayer hopping a BG for commensurate angles, due to the presence of inter-layer interactions [29].

In this paper, we investigate the ground-state proper-

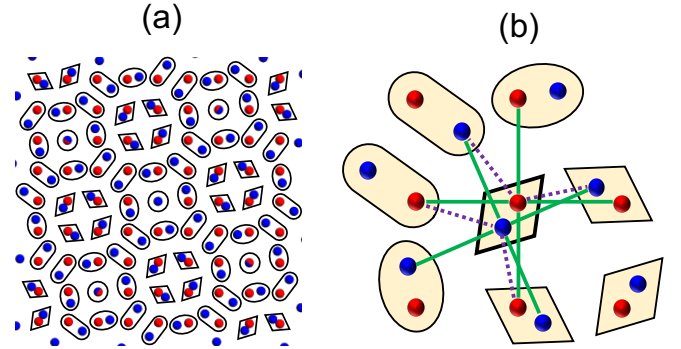


FIG. 1. (a) Twisted-bilayer lattice for a moiré angle $\theta = \theta(3,2)$. Sites of layer 1 (2) are indicated by filled red (blue) circles. We indicate with different forms the different cluster types: cluster 1 (circle), 2 (rhombus), 3 (oval) and 4 (rounded rectangle). These clusters are characterized by different inter-layer couplings, see text. For this lattice there are no unclustered sites. (b) Hopping between neighboring clusters results from intra-layer (inter-layer) tunneling indicated with solid-green (dashed-purple) lines.

ties of interacting ultra-cold bosons in a twisted-bilayer optical lattice. Due to inter-layer tunneling, the lattice splits into clusters of two sites, each one belonging to a different layer, which are connected by a significant inter-layer hopping. We develop a specific Gutzwiller Ansatz that takes properly into account clusterization. Equipped with this method, we show that the interplay between interactions and the twist-induced lattice clusterization results in a rich ground-state physics, for both commensurate and incommensurate twistings. Mott-like phases are characterized by a non-trivial dependence of the filling of the different clusters with the chemical potential, resulting typically in a density wave modulation. Bose-glass phases may occur even for commensurate angles due to the formation of “quantum wheels” similar to those observed in quasi-crystals in Ref. [26]. For in-

commensurate twistings, the Bose glass is characterized by the formation of non-trivial isolated domains of sites, in between which particles may freely move. For sufficiently large hopping amplitudes, the eventual percolation of these islands leads to a superfluid phase [25, 30].

The paper is organized as follows. In Sec. II we introduce the model, the cluster Gutzwiller approach employed throughout the paper, as well as the percolation analysis. Section III is devoted to the case of commensurate twistings and the formation of mobility islands. Section IV deals with incommensurate twisting angles, discussing separately the case with and without inter-layer hopping. Finally, in Sec. V we summarize our conclusions.

II. MODEL AND METHODS

A. Hamiltonian

In the following, we consider contact-interacting bosons in two layers of square optical lattices, where one layer is twisted by an angle θ with respect to the other. We focus in particular on the case in which this arrangement is engineered in the way proposed in Ref. [13], and recently realized experimentally in Ref. [20], in which two internal levels of the atoms act as two effective layers in a synthetic dimension, whereas a state-dependent potential results in the twisted-bilayer geometry. For a square lattice geometry, a periodic moiré pattern is obtained for twist angles $\theta = \theta(m, n) \equiv \arccos(\frac{2mn}{m^2+n^2})$ ($n, m \in \mathbb{Z}$). The Hamiltonian of the system acquires the form:

$$\begin{aligned} H = & -t \sum_{\alpha} \sum_{\langle j, j' \rangle} a_{\alpha, j}^{\dagger} a_{\alpha, j'} - \sum_{\alpha \neq \bar{\alpha}} \sum_{j, j'} t_{\perp}(j, j') a_{\alpha, j}^{\dagger} a_{\bar{\alpha}, j'} \\ & + \frac{U}{2} \sum_{\alpha} \sum_j \hat{n}_{\alpha, j} (\hat{n}_{\alpha, j} - 1) - \mu \sum_{\alpha} \sum_j \hat{n}_{\alpha, j} \\ & + \sum_{\alpha} \sum_{j, j'} V_{\perp}(j, j') \hat{n}_{\alpha, j} \hat{n}_{\bar{\alpha}, j'} \end{aligned} \quad (1)$$

where $a_{\alpha, j}$ ($a_{\alpha, j}^{\dagger}$) is the annihilation (creation) operator at site j of layer $\alpha = \{1, 2\}$, $\hat{n}_{\alpha, j} = \hat{a}_{\alpha, j}^{\dagger} \hat{a}_{\alpha, j}$, U characterizes the on-site repulsive interactions, assumed to be the same in both layers, and μ is the chemical potential. Note that whereas intra-layer hopping to nearest neighbors is given by a fixed hopping rate t , tunneling between a site j in one layer and site j' in the opposite one is characterized by the variable rate $t_{\perp}(j, j')$. The repulsive inter-layer interactions are given by the couplings $V_{\perp}(j, j')$. In the considered scenario using synthetic dimensions, intra-layer hopping results from either a microwave or two-photon optical Raman coupling between the two internal levels, whereas inter-layer interactions result from contact-like interactions between the two internal components. For a sufficiently deep optical lattice, the on-site Wannier functions (in each layer) can be approximated as a Gaussian of width $l_0 = \frac{a}{\pi s^{1/4}}$, where a

is the lattice spacing characterizing the square lattice in both layers, and s is the lattice depth in recoil units. As a result, the distance-dependent inter-layer hopping and interaction acquire, respectively, the form [13]: $t_{\perp}(j, j') = t_{\perp} e^{-|R_{1j} - R_{2j'}|^2 / 4l_0^2}$, and $V_{\perp}(j, j') = V_{\perp} e^{-|R_{1j} - R_{2j'}|^2 / 2l_0^2}$. We have chosen $l_0 = 0.15a$ ($s \simeq 20$) throughout the paper. Note that t_{\perp} can be controlled by the strength and detuning of the coupling between internal levels, whereas V_{\perp} depends on the contact-like inter-component interactions.

B. Site clusterization

Due to the twisting between the two lattices, and the Gaussian dependence of the inter-layer hopping, sites at different positions present a markedly different coupling to sites in the opposite layer. In particular, pairs of neighboring sites i and j may present a significant inter-layer hopping $t_{\perp}(i, j)$, much stronger than the inter-layer coupling to any other site. Moreover, for sufficiently low t , $t_{\perp}(i, j)$ may overwhelm as well the intra-layer tunneling. When this occurs, in first approximation, those two sites could be then considered as a cluster decoupled from the rest of the lattice, forming an effective two-well potential. As a result, a single particle in those two sites would occupy in the ground-state the symmetric superposition $(|i\rangle + |j\rangle)/\sqrt{2}$ with energy $-t_{\perp}(i, j)$. Although this decoupling is generally not exact, and inter-cluster hopping plays a relevant role (as depicted in Fig. 1 (b)), site clusterization turns out to be crucial to understand the ground-state physics of the interacting Bose gas in the twisted bilayer lattice.

We define a cluster c as formed by two sites c_1 and c_2 , in layers 1 and 2, respectively, such that $t_{\perp}(c_1, c_2) > t_{\perp, cr}$. In the following, we set $t_{\perp, cr} = 0.03$ (0.06) t_{\perp} for commensurate (incommensurate) twist angles. We have checked that lower values of $t_{\perp, cr}$ do not appreciable change the results discussed below. Note that due to the Gaussian dependence of the inter-layer tunneling, for all values of t_{\perp} discussed in this paper, clusters are always limited to two sites. In addition to the clustered (cl) states, there may be also sites without a significant coupling to any neighboring site in the opposite ladder. They do not belong to a cluster, and are referred below as non-clustered (ncl) sites. For the case of a given moiré angle, the clusters can be classified in well-defined types, characterized by a different inter-layer coupling. The case of $\theta = \theta(3, 2)$ is shown in Fig. 1 (a), where we indicate the different cluster types. As discussed below, coupling between neighboring clusters via intra- and inter-layer tunneling, illustrated in Fig. 1 (b), plays a key role in the eventual on-set of superfluidity in the lattice.

Motivated by the previous discussion, we introduce the Gutzwiller-like ansatz $|\Psi\rangle = |\Psi_{cl}\rangle \otimes |\Psi_{ncl}\rangle$. Clustered sites are described by $|\Psi_{cl}\rangle = \bigotimes_{c \in cl} |\rho_c^{cl}\rangle$, with $|\rho_c^{cl}\rangle = \sum_{n_1, n_2} g_c(n_1, n_2) |n_1\rangle_{c_1} |n_2\rangle_{c_2}$, where $g_c(n_1, n_2)$

determines the amplitude of probability of finding n_1 (n_2) particles in site c_1 (c_2) of cluster c . Non-clustered sites are characterized by $|\Psi_{ncl}\rangle = \bigotimes_{\alpha,j \in ncl} |\rho_{\alpha,j}\rangle$, with $|\rho_{\alpha,j}\rangle = \sum_n f_{\alpha,j}(n) |n\rangle_{\alpha,j}$, where $f_{\alpha,j}(n)$ is the amplitude of probability of finding n particles in the non-clustered site j of layer α . The coefficients fulfill the normalization conditions: $\sum_n |f_{\alpha,j}(n)|^2 = \sum_{n_1, n_2} |g_c(n_1, n_2)|^2 = 1$.

An uncoupled non-clustered site (α, j) is characterized by an energy:

$$\tilde{E}_{(\alpha,j)} = \sum_n \epsilon(n) |f_{\alpha,j}(n)|^2, \quad (2)$$

with $\epsilon(n) = \frac{U}{2}n(n-1) - \mu n$, whereas the energy of an uncoupled cluster c is:

$$E_c = \sum_{n_1, n_2} \xi_c(n_1, n_2) |g_c(n_1, n_2)|^2 - t_{\perp, c} \sum_{n_1, n_2} \left(\sqrt{n_1(n_2+1)} g_c^*(n_1, n_2) g_c(n_1-1, n_2+1) + \text{c.c.} \right), \quad (3)$$

with $t_{\perp, c}$ and $V_{\perp, c}$ characterizing the inter-layer couplings in the cluster, and $\xi_c(n_1, n_2) = \sum_{\sigma=1,2} \epsilon(n_\sigma) + V_{\perp, c} n_1 n_2$.

Neglecting interactions between different clusters or unclustered sites (which is extremely small under the conditions discussed below), coupling between clusters is only given by hopping. Intra-layer hopping between neighboring clusters c and c' result in the energy $T_{c,c'}^{\text{intra}} = -t \sum_{\alpha} (b_{\alpha, c_\alpha}^* b_{\alpha, c'_\alpha} + \text{c.c.})$, if c_α and c'_α are nearest neighbors in layer α , whereas inter-layer tunneling results in the contribution: $T_{c,c'}^{\text{inter}} = -t_{\perp} (c_\alpha, c'_\alpha) (b_{\alpha, c_\alpha}^* b_{\alpha, c'_\alpha} + \text{c.c.})$. Similarly, the hopping between two neighboring ncl sites contributes with $T_{(\alpha,i),(\alpha,j)}^{\text{intra}} = -t b_{\alpha,i}^* b_{\alpha,j} + \text{c.c.}$, and $T_{(1,i),(2,j)}^{\text{inter}} = -t_{\perp} (i, j) b_{1,i}^* b_{2,j} + \text{c.c.}$. Finally, hops between clustered and non-clustered sites result, respectively, in couplings $T_{(\alpha,c),(\alpha,j)}^{\text{intra}} = -t b_{\alpha,c}^* b_{\alpha,j} + \text{c.c.}$, where c_α and j are nearest neighbors, and $T_{(\alpha,c),(\bar{\alpha},j)}^{\text{inter}} = -t_{\perp} (c_\alpha, j) (b_{\alpha,c}^* b_{\bar{\alpha},j} + \text{c.c.})$. In the previous expressions we have introduced the mean-fields: $b_{\alpha,c \in \text{cl}} \equiv \langle \hat{a}_{\alpha,c} \rangle$ and $b_{(\alpha,j) \in \text{ncl}} \equiv \langle \hat{a}_{\alpha,j} \rangle$, which are determined from the Gutzwiller coefficients:

$$b_{1,c} = \sum_{n_1, n_2} \sqrt{n_1+1} g_c^*(n_1, n_2) g_c(n_1+1, n_2), \quad (4)$$

$$b_{2,c} = \sum_{n_1, n_2} \sqrt{n_2+1} g_c^*(n_1, n_2) g_c(n_1, n_2+1), \quad (5)$$

$$b_{\alpha,j} = \sum_n \sqrt{n+1} f_{\alpha,j}^*(n) f_{\alpha,j}(n+1). \quad (6)$$

Adding up all the energy terms, we obtain the overall energy E , which we minimize obtaining the coefficients $g_c(n_1, n_2)$ and $f_{\alpha,j}(n)$.

C. Percolation analysis

In Bose-Hubbard models in uniform square lattices, the superfluid (SF) phase is characterized by a non-zero

mean-field $\langle \hat{a}_j \rangle$ in all sites j , whereas a Mott-like insulator (MI) present a zero mean-field and an integer $\langle \hat{n}_j \rangle$. In the twisted-bilayer scenario, sites belonging to different clusters (or sites in non-cluster states) typically present different fillings and different values of the mean fields $b_{\alpha,s}$. As discussed below, this leads to a rich landscape of possible phases.

Due to the inherent inhomogeneity of twisted-bilayer lattices, some sites may present a vanishing mean-field, whereas others may have a non-vanishing one. In our analysis, we fix the cut-off $|b_{\alpha,s}| < 0.05$ to determine whether a site has a vanishing mean-field. We associate at this point the parameter $S = 1$ (0) to each site with non-vanishing (vanishing) mean-field.

We define a Mott-like phase as having $S = 0$ for all sites, and hence clusters with an integer filling. Note however that different clusters can have different integer fillings, hence resulting rather in a density wave. When at least some sites present $S = 1$, superfluidity is only established if $S = 1$ sites percolate [25, 30, 31]. We determine the network of sites formed by connecting all the nearest-neighboring (both intra- and inter-layer) sites with $S = 1$. We consider two $S = 1$ sites as connected if their coupling is larger than $10^{-3} t_{\perp}$. A slight change of this value does not affect any of our results. We then employ a percolation analysis, based on the Hoshen-Kopelman algorithm [32], to determine whether there is at least one chain of $S = 1$ sites that percolates from one side to the other of our system. Note that although percolation may not occur, there may be a significant fraction of neighboring sites with $S = 1$, which will then form an isolated superfluid region. This phase, as discussed below, may occur even in the case of commensurate moiré angles.

Motivated by the previous discussion, and following Refs. [25, 30], we introduce two further parameters: the fraction of $S = 1$ sites $F \equiv N_{\phi}/N$, and the percolation probability $P \equiv N_{\text{span}}/N$, where N_{span} , N_{ϕ} and N denote, respectively, the number of $S = 1$ sites in a percolating chain, the total number of $S = 1$ sites, and total number of sites in the two layers. Mott-like phases are characterized by $F = P = 0$, whereas for the SF phase $F, P > 0$. Non-percolated phases with $\langle S \rangle > 0$ present $P = 0$ but $F > 0$. In the following, and due to their resemblance with the Bose glass phase known in disorder Bose-Hubbard models [22], we denote these phases as BG phases.

III. COMMENSURATE TWIST ANGLE

We consider first the case of a commensurate twist angle $\theta = \theta(m, n)$. We may then simplify our analysis by using periodic boundary conditions (PBC), focusing on a single unit cell of the effective moiré lattice. We illustrate the possible ground-state phases of the interacting Bose gas with the case of $\theta = \theta(3, 2)$, since it presents already a complex landscape of clusters, but the different phases are still intuitively easy to visualize. The

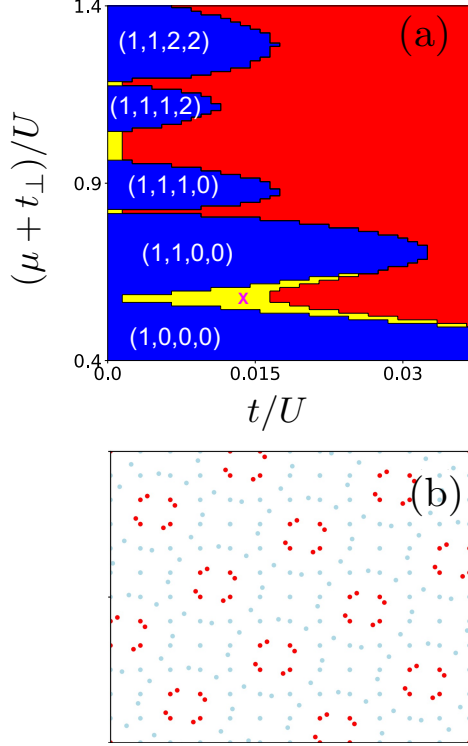


FIG. 2. (a) Phase diagram for $\theta = \theta(3, 2)$, $l_0 = 0.15a$, $t_\perp = U$, and $V_\perp = 4U$. Insulating Mott-like phases are indicated in blue, SF phases in red, and BG phases in yellow. The Mott-like phases are labelled in the form (N_1, N_2, N_3, N_4) , where N_c is the population of cluster c (see Fig. 1). (b) Distribution of sites with $S = 1$ (red) and $S = 0$ (light blue) characteristic of the BG phase in between $(1, 0, 0, 0)$ and $(1, 1, 0, 0)$ (for the case indicated with a cross in Fig. (a)).

lattice presents four different cluster types, $c = 1 \dots 4$, see Fig. 1. Clusters 1 (circles) are formed by two sites on top of each other, and hence $t_{\perp, c=1}/t_\perp = 1$. The rest of the clusters present a lower inter-layer coupling: cluster 2 (rhombuses) present $t_{\perp, 2}/t_\perp \simeq 0.425$, cluster 3 (ovals) $t_{\perp, 3}/t_\perp \simeq 0.181$, and cluster 4 (rounded rectangles) $t_{\perp, 4}/t_\perp \simeq 0.033$.

Figure 2 (a) shows the phase diagram for $t_\perp = U$, and $V_\perp = 4U$ (other choices lead to qualitatively similar phase diagrams). The Mott-like phases (indicated in blue) are characterized by an integer, generally different, population N_c of the different cluster types. We denote these phases in the form (N_1, N_2, N_3, N_4) .

At low chemical potential, the lattice is first filled with one particle in each cluster 1, due to the strong inter-layer hopping rate in these clusters. Increasing the chemical potential results in the filling of other clusters, starting with cluster 2. Note however that the transition between the $(1, 0, 0, 0)$ and $(1, 1, 0, 0)$ phases occurs at low t/U via an intermediate phase, illustrated in Fig. 2 (b), in which

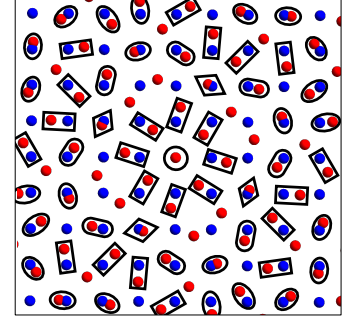


FIG. 3. Spatial distribution of sites in layer 1 (blue) and layer 2 (red) for a lattice with an angle $\theta(2, 1) + 3^\circ$. For simplicity, in addition to the two central overlapping sites (circle), we classify the rest of the clusters in four families: 1 (rhombuses), 2 (ovals), 3 (rounded rectangles), and 4 (rectangles). Note also the presence of non-clustered sites.

the dc sites have unit filling, but clusters 2 form superfluid ring islands, which resemble the quantum wheels recently reported in the context of quasi-crystal potentials [26]. These islands remain however isolated, without percolating through the lattice. As a result the system is in a BG phase (indicated in yellow), with $P = 0$ but $F > 0$. At larger t/U the coupling with clusters 3 eventually results in a percolating network of clusters 2 and 3, and hence the system enters the SF phase (red). Larger values of the chemical potential result in a non-trivial series of Mott-like phases, in which the filling is not necessarily sequential, e.g. $(1, 1, 1, 0)$ is followed by $(1, 1, 1, 2)$, with an appreciable gap in between. Concerning that gap, note that even if $t = 0$, mobility can be established exclusively via inter-layer hops, explaining the absence of Mott phases at $t/U = 0$ when $(\mu + t_\perp)/U \simeq 1$.

IV. INCOMMENSURATE TWIST ANGLE

We consider next the case of incommensurate twist angles. Since the lattice lacks periodicity, we cannot employ periodic boundary conditions and must hence work with finite-size systems. Inter-layer clusters of two neighboring sites may still be formed. Sites which experience an inter-layer coupling $t_{\perp, c} > 0.06t_\perp$ are considered as belonging to the same cluster. This cut-off value prevents in the cases discussed below the existence of clusters of more than two sites, without compromising the generality of the results. Sites which experience an interlayer coupling below that cut-off are considered as non-clustered sites. Our numerical simulation is performed on a 40×40 twisted bilayer optical lattice.

In the following, we illustrate the possible ground-state phases for the case of incommensurate twist angles, using the relatively simple case of $\theta = \theta(2, 1) + 3^\circ$, see Fig. 3. By construction, there is one site in the middle of each layer forming a single cluster with coupling t_\perp . In contrast to the commensurate case, in the in-

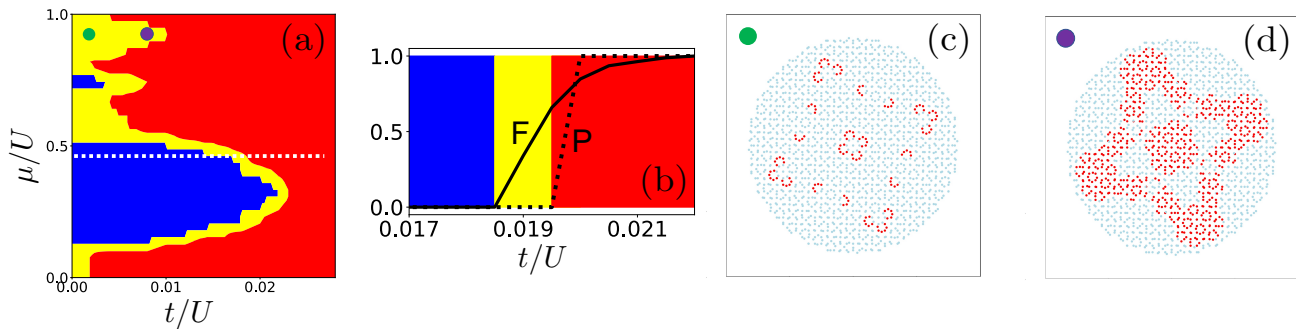


FIG. 4. (a) Phase diagram for $\theta = \theta(2, 1) + 3^\circ$, $t_\perp/U = 1$, and $V_\perp = 0$. Insulating Mott-like phases are indicated in blue, BG phases in yellow, and superfluid phases in red. (b) the F (solid line) and P (dashed line) parameters (see text) as a function of t/U for $\mu/U = 0.45$. These parameters are employed to characterize the phases. (c)-(d) distribution of sites with $S = 1$ (red) and $S = 0$ (light blue) for the cases indicated in (a). We choose 40×40 sites in each layer.

commensurate case, due to the aperiodicity of the lattice, the other two-site clusters present generally different inter-layer couplings. In order to simplify the analysis, we classify the clusters into four families, with respectively $t_{\perp, c=1\dots 4}/t_\perp \in [0.75, 1)$, $[0.5, 0.75)$, $[0.2, 0.5)$, and $[0.06, 0.2)$, respectively. We then assign to the clusters in each family the average value within the family, i.e. $t_{\perp, c=1\dots 4}/t_\perp = 0.875, 0.625, 0.35$, and 0.013 . Slightly different choices of these cluster families do not change the qualitative picture discussed below.

We consider first the case $V_\perp = 0$ and $t_\perp = U$, see Fig. 4. The ground-state phase diagram in this case is characterized by a broad Mott insulator regime with one particle in all sites, separated from the SF regime by a BG region. For larger chemical potentials, we observe the appearance of a wide BG regime at low t/U , which almost completely wipes out any other Mott-like insulating lobes. That regime is characterized at low t/U by the formation of small pockets of sites with $S = 1$, formed by sites in clusters $c = 4$ and unclustered sites, see Fig. 4 (c). Note that even at $t = 0$, there may be pockets of sites in which particles can move. This is because motion between sites may be established solely by inter-layer hops. When t/U increases, inside the BG phase, larger (but still disconnected) regions with $S = 1$ form [see Fig. 4 (d)]. As a result in the BG phase, $F > 0$, but $P = 0$, i.e. there is no overall percolation of the $S = 1$ sites, see Fig. 4 (b). For an even larger t/U the system eventually enters the SF phase with percolated $S = 1$ sites (a more clear example of this is discussed below). The phase diagram resembles qualitatively that obtained for strongly disordered Bose-Hubbard models [22].

We discuss at this point a different scenario, in which the layers are not coherently coupled, i.e. there is no interlayer hopping ($t_\perp = 0$). We consider, however, $V_\perp \neq 0$. We show in the following that interlayer interactions may result as well in a rich ground-state phase diagram. In the absence of inter-layer coupling, we may carry on with the idea of clusterization but classifying the clusters (still formed by only two sites) according to the inter-layer interaction strength between their sites.

Note that for commensurate twist angles, unless they are very small, interlayer interactions, which decay much faster than the inter-layer hopping with distance, are typically very weak, except for the case of sites placed on top of each other. As a result, the layers behave as almost disconnected in the absence of interlayer hopping, except for the sites which are on top of each other, in which particles may become disconnected from the rest of the lattice if $V_\perp \gg t$. Excluding these sites, however does not result in disconnected regions in each layer, and hence it does not affect the overall mobility in the lattice. As a result BG is not observed. We note that for very small twist angles, interactions may outproject more sites in the lattice at each layer, and as a result a BG may occur, as recently reported in Ref. [29]

In contrast, even for large angles, incommensurate twist angles result in sites which may be eventually close enough to experience significant interlayer interactions, and as result, for aperiodic lattices interlayer interactions do significantly affect the phase diagram, even for $t_\perp = 0$, resulting in a rich ground-state physics. We illustrate this physics again for the case of $\theta(2, 1) + 3^\circ$, with $t_\perp = 0$ and $V_\perp/U = 1$, see Fig. 5 (a).

As for the case of interlayer hopping, pairs of neighboring sites in each layer present very different interlayer interactions across the lattice. We hence split the sites into different cluster families, according to their interlayer interactions, into 5 families with $V_{\perp, c=1\dots 5}/V_\perp \in 1$, $[0.75, 1)$, $[0.5, 0.75)$, $[0.2, 0.5)$, and $[0.06, 0.2)$. As for the case with $t_\perp > 0$ we characterized the phases with the parameters F and P , discussed above. For the case considered we observe several Mott-like insulating phases, which we characterized by the number of particles per site in the different clusters. The three largest Mott-like regions are characterized, from bottom to top, by populations $(1, 1, 1, 2, 2)$, $(1, 1, 2, 2, 2)$, and $(1, 2, 2, 2, 2)$. Note that the clusters with lower interlayer interactions are more populated, as expected due to the repulsive character of the interactions. The BG regime completely surrounds the Mott-like regions, separating them from the SF regime. Note that mobility results exclusively from

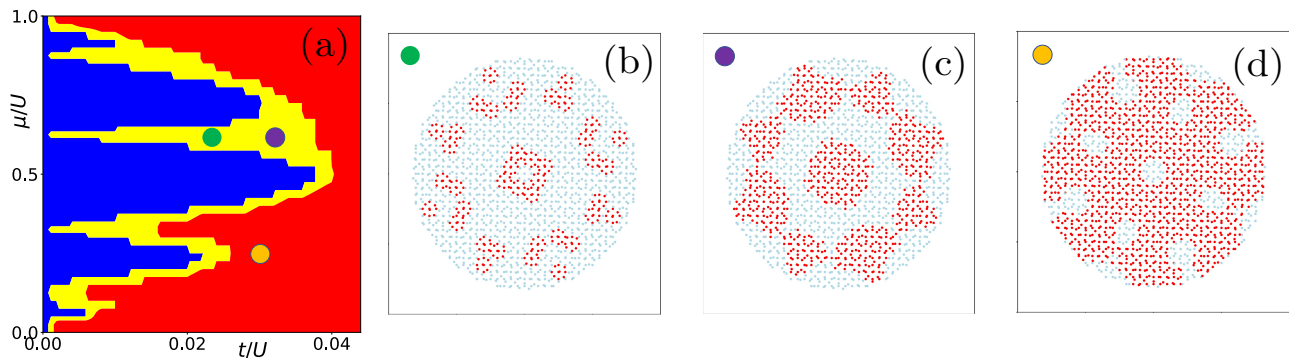


FIG. 5. (a) Phase diagram for $\theta = \theta(2,1) + 3^\circ$, $V_\perp/U = 1$, and $t_\perp = 0$. Insulating Mott-like phases are indicated in blue, BG phases in yellow, and superfluid phases in red. (b)–(d) Distribution of the sites with $S = 1$ (red) and $S = 0$ (blue), for the cases indicated in (a) by the colored circles.

intra-layer hops, and hence in contrast to the case of finite t_\perp , at $t = 0$ no mobility is possible and the phase diagram is dominated by the Mott-like regions. Figs 5 (b) and (c) show the spatial distribution of $S = 1$ sites within the BG regime. For growing t/U the islands of sites in which particles can move become larger, although in the BG regime they remain disconnected. In the SF regime, the regions with $S = 1$ percolate, but islands of insulating sites (which do not participate in particle transport) remain in the system, see Fig. 5 (d). The latter case is characterized by $P = 1$ (i.e. percolation), but $F < 1$, i.e. not all sites have $S = 1$.

V. CONCLUSIONS

Cold atoms in twisted-bilayer optical potentials constitute an excellent platform for the study of the interplay of interactions and the twisted geometry, since they present vastly tunable parameters, a feature typically not shared by the solid-state implementation of similar setups. Our results illustrate the rich and highly non-trivial ground-state physics introduced by interactions in twisted-bilayer-like optical lattices, which results from the interplay between inter- and intra-layer hopping and interactions. Crucially, inter-layer hopping induces the formation of two-site clusters, which we have prop-

erly taken into account by means of a specifically tailored cluster Gutzwiller approach. For commensurate twist angles (periodic lattices) regular cluster families with different interlayer couplings are formed. Cluster formation results in a rich variety of Mott-like phases. Moreover, even for periodic lattices, Bose-glass-like phases occur in which particles can move in between specific sites forming isolated pockets, without establishing an overall superfluidity. The BG-like regime is significantly more relevant in the case of incommensurate twistings (aperiodic lattice). Interestingly, for that case (but not for the commensurate one, at least for large angles), highly non-trivial BG-like and superfluid phases may result exclusively from interlayer interactions, even in the absence of interlayer hopping. Although we have focused on ground-state properties, a highly non-trivial dynamics is also expected in these setups, which may be studied as well using the introduced cluster Gutzwiller formalism.

ACKNOWLEDGMENTS

GCP thanks Dean Johnstone for discussion regarding percolation analysis. We acknowledge support of the Deutsche Forschungsgemeinschaft (DFG, German Research Foundation) under Germany's Excellence Strategy – EXC-2123 Quantum-Frontiers – 390837967.

-
- [1] R. Bistritzer and A. H. MacDonald, Moiré bands in twisted double-layer graphene, *Proc. of the National Academy of Sciences* **108**, 12233 (2011).
 - [2] E. Y. Andrei and A. H. MacDonald, Graphene bilayers with a twist, *Nature materials* **19**, 1265 (2020).
 - [3] G. Tarnopolsky, A. J. Kruchkov, and A. Vishwanath, Origin of magic angles in twisted bilayer graphene, *Phys. Rev. Lett.* **122**, 106405 (2019).
 - [4] Y. Cao, V. Fatemi, S. Fang, K. Watanabe, T. Taniguchi, E. Kaxiras, and P. Jarillo-Herrero, Unconventional super-

conductivity in magic-angle graphene superlattices, *Nature* **556**, 43 (2018).

- [5] M. Yankowitz, S. Chen, H. Polshyn, Y. Zhang, K. Watanabe, T. Taniguchi, D. Graf, A. F. Young, and C. R. Dean, Tuning superconductivity in twisted bilayer graphene, *Science* **363**, 1059 (2019).
- [6] M. Oh, K. P. Nuckolls, D. Wong, R. L. Lee, X. Liu, K. Watanabe, T. Taniguchi, and A. Yazdani, Evidence for unconventional superconductivity in twisted bilayer graphene, *Nature* **600**, 240 (2021).

- [7] M. Yankowitz, S. Chen, H. Polshyn, Y. Zhang, K. Watanabe, T. Taniguchi, D. Graf, A. F. Young, and C. R. Dean, Tuning superconductivity in twisted bilayer graphene, *Science* **363**, 1059 (2019).
- [8] Y. Cao, V. Fatemi, A. Demir, S. Fang, S. L. Tomarken, J. Y. Luo, J. D. Sanchez-Yamagishi, K. Watanabe, T. Taniguchi, E. Kaxiras, *et al.*, Correlated insulator behaviour at half-filling in magic-angle graphene superlattices, *Nature* **556**, 80 (2018).
- [9] E. Codecido, Q. Wang, R. Koester, S. Che, H. Tian, R. Lv, S. Tran, K. Watanabe, T. Taniguchi, F. Zhang, *et al.*, Correlated insulating and superconducting states in twisted bilayer graphene below the magic angle, *Science Adv.* **5**, eaaw9770 (2019).
- [10] K. P. Nuckolls, M. Oh, D. Wong, B. Lian, K. Watanabe, T. Taniguchi, B. A. Bernevig, and A. Yazdani, Strongly correlated chern insulators in magic-angle twisted bilayer graphene, *Nature* **588**, 610 (2020).
- [11] Y. Cao, D. Rodan-Legrain, O. Rubies-Bigorda, J. M. Park, K. Watanabe, T. Taniguchi, and P. Jarillo-Herrero, Tunable correlated states and spin-polarized phases in twisted bilayer-bilayer graphene, *Nature* **583**, 215 (2020).
- [12] D. Shechtman, I. Blech, D. Gratias, and J. W. Cahn, Metallic phase with long-range orientational order and no translational symmetry, *Phys. Rev. Lett.* **53**, 1951 (1984).
- [13] A. González-Tudela and J. I. Cirac, Cold atoms in twisted-bilayer optical potentials, *Phys. Rev. A* **100**, 053604 (2019).
- [14] T. Salamon, A. Celi, R. W. Chhajlany, I. Frérot, M. Lewenstein, L. Tarruell, and D. Rakshit, Simulating twistorics without a twist, *Phys. Rev. Lett.* **125**, 030504 (2020).
- [15] X.-W. Luo and C. Zhang, Spin-twisted optical lattices: tunable flat bands and larkin-ovchinnikov superfluids, *Phys. Rev. Lett.* **126**, 103201 (2021).
- [16] J. Lee and J. Pixley, Emulating twisted double bilayer graphene with a multiorbital optical lattice, *SciPost Physics* **13**, 033 (2022).
- [17] C. Madroño and R. Paredes, Dynamic stability in spinor bose gases in moiré lattices with square and hexagonal symmetries, *Phys. Rev. A* **107**, 033316 (2023).
- [18] G. C. Paul, P. Recher, and L. Santos, Particle dynamics and ergodicity breaking in twisted-bilayer optical lattices, *Phys. Rev. A* **108**, 053305 (2023).
- [19] X.-T. Wan, C. Gao, and Z.-Y. Shi, Fractal spectrum in twisted bilayer optical lattice, *arXiv preprint arXiv:2404.08211* (2024).
- [20] Z. Meng, L. Wang, W. Han, F. Liu, K. Wen, C. Gao, P. Wang, C. Chin, and J. Zhang, Atomic bose-einstein condensate in twisted-bilayer optical lattices, *Nature* **615**, 231 (2023).
- [21] M. Greiner, O. Mandel, T. Esslinger, T. W. Hänsch, and I. Bloch, Quantum phase transition from a superfluid to a mott insulator in a gas of ultracold atoms, *Nature* **415**, 39 (2002).
- [22] M. P. Fisher, P. B. Weichman, G. Grinstein, and D. S. Fisher, Boson localization and the superfluid-insulator transition, *Phys. Rev. B* **40**, 546 (1989).
- [23] P. Lugan, D. Clément, P. Bouyer, A. Aspect, M. Lewenstein, and L. Sanchez-Palencia, Ultracold bose gases in 1d disorder: From lifshits glass to bose-einstein condensate, *Phys. Rev. Lett.* **98**, 170403 (2007).
- [24] L. Fallani, J. Lye, V. Guarrera, C. Fort, and M. Inguscio, Ultracold atoms in a disordered crystal of light: Towards a bose glass, *Phys. Rev. Lett.* **98**, 130404 (2007).
- [25] D. Johnstone, P. Öhberg, and C. W. Duncan, The mean-field bose glass in quasicrystalline systems, *J. Phys. A: Math. Theor.* **54**, 395001 (2021).
- [26] M. Ciardi, A. Angelone, F. Mezzacapo, and F. Cinti, Quasicrystalline bose glass in the absence of disorder and quasidisorder, *Phys. Rev. Lett.* **131**, 173402 (2023).
- [27] J.-C. Yu, S. Bhave, L. Reeve, B. Song, and U. Schneider, Observing the two-dimensional bose glass in an optical quasicrystal, *Nature* **633**, 338 (2024).
- [28] D. Johnstone, S. Mishra, Z. Zhu, H. Yao, and L. Sanchez-Palencia, Weak superfluidity in twisted optical potentials, *arXiv preprint arXiv:2406.12963* (2024).
- [29] J.-H. Zeng, Q. Zhu, and L. He, Dynamical moiré systems in twisted bilayer optical lattices, *arXiv preprint arXiv:2405.20732* (2024).
- [30] A. Niederle and H. Rieger, Superfluid clusters, percolation and phase transitions in the disordered, two-dimensional bose-hubbard model, *New J. of Phys.* **15**, 075029 (2013).
- [31] K. Hettiarachchilage, C. Moore, V. Rousseau, K.-M. Tam, M. Jarrell, and J. Moreno, Local density of the bose-glass phase, *Phys. Rev. B* **98**, 184206 (2018).
- [32] J. Hoshen and R. Kopelman, Percolation and cluster distribution. i. cluster multiple labeling technique and critical concentration algorithm, *Phys. Rev. B* **14**, 3438 (1976).